Chemistry & Biology
Article

Discovery of 23 Natural Tubulysins from *Angiococcus disciformis* An d48 and *Cystobacter* SBCb004

Yi Chai,[1,4] Dominik Pistorius,[1,4] Angelika Ullrich,[2] Kira J. Weissman,[1] Uli Kazmaier,[2] and Rolf Müller[1,3,*]
[1]Department of Pharmaceutical Biotechnology, Saarland University, P.O. Box 151150, 66041 Saarbrücken, Germany
[2]Institute for Organic Chemistry, Saarland University, 66123 Saarbrücken, Germany
[3]Helmholtz Institute for Pharmaceutical Research Saarland (HIPS), Helmholtz Center for Infection Research (HZI), Saarland University, Campus C2 3, 66123 Saarbrücken, Germany
[4]These authors contributed equally to this work
*Correspondence: rom@mx.uni-saarland.de
DOI 10.1016/j.chembiol.2010.01.016

SUMMARY

The tubulysins are a family of complex peptides with promising cytotoxic activity against multi-drug-resistant tumors. To date, ten tubulysins have been described from the myxobacterial strains *Angiococcus disciformis* An d48 and *Archangium gephyra* Ar 315. We report here a third producing strain, *Cystobacter* sp. SBCb004. Comparison of the tubulysin biosynthetic gene clusters in SBCb004 and An d48 reveals a conserved architecture, allowing the assignment of cluster boundaries. A SBCb004 strain containing a mutant in the putative cyclodeaminase gene *tubZ* accumulates pretubulysin A, the proposed first enzyme-free intermediate in the pathway, whose structure we confirm by NMR. We further show, using a combination of feeding studies and structure elucidation by NMR and high-resolution tandem mass spectrometry, that SBCb004 and An d48 together biosynthesize 22 additional tubulysin derivatives. These data reveal the inherently diversity-oriented nature of the tubulysin biosynthetic pathway.

INTRODUCTION

The tubulysins are highly cytotoxic compounds, whose growth inhibition potential exceeds that of the anticancer drugs epothilone, vinblastine, and taxol, by 20–1000 fold (Steinmetz et al., 2004). The metabolites are active against a wide variety of cancer cell lines (ovarian, breast, prostate, colon, lung, and leukemia) within the NIC-60 cell line panel, including multi-drug-resistant tumors (Dömling and Richter, 2005). Mode-of-action studies have demonstrated that the tubulysins disrupt microtubule assembly (Khalil et al., 2006), and also show antiangiogenic effects (Kaur et al., 2006). Together, these properties make the tubulysins attractive lead structures for development as antineoplastic agents.

The nine-membered tubulysin family was discovered by Höfle, Reichenbach, and coworkers from several myxobacterial strains including *Angiococcus disciformis* An d48, and *Archangium gephyra* Ar 315, using bioactivity-guided screening (Sasse et al., 2000; Steinmetz et al., 2004). The shared molecular core comprises five amino acids (*N*-methyl pipecolic acid [Mep], isoleucine [Ile], valine, cysteine, and phenylalanine or tyrosine), and two units of acetate (Figure 1D). In the synthetic literature, valine, cysteine, and one unit of acetate have been grouped together into a structural unit referred to as tubuvaline (Tuv), whereas the acetate chain-extended forms of phenylalanine or tyrosine are designated as tubuphenylalalaline (Tup) and tubutyrosine (Tut), respectively. All of the structures include an acetoxy moiety, but exhibit variable functionality (R^2) within the Tuv bis-acyl *N*,*O*-acetal substituent (Figure 1D). SAR studies using synthetic analogs of the most potent tubulysin, tubulysin D (**1**), have begun to define the structural features underlying the compound's cytotoxicity (Patterson et al., 2007; Balasubramanian et al., 2008; Raghavan et al., 2008; Wang et al., 2007; Patterson et al., 2008). Taken together, these data reveal a surprising tolerance to structural modification, encouraging efforts to synthesize simplified variants of the tubulysins for evaluation as anticancer agents. For example, replacing the chemically labile *N*,*O*-acetal and stereogenic acetate groups of tubuvaline with stable alternatives, resulted in only a minor loss of potency (Raghavan et al., 2008). As a complement to chemical synthesis, we have aimed to enable the genetic engineering of additional tubulysin analogs by detailed investigation of the underlying biosynthetic machinery (Sandmann et al., 2004; Wenzel and Müller, 2005; Bode and Müller, 2006; Wenzel and Müller, 2007).

Angiococcus disciformis An d48 is known to produce four tubulysins, tubulysins D (**1**), E (**2**), F (**3**), and H (**4**) (Steinmetz et al., 2004). Sequencing of the ca. 40 kb tubulysin gene cluster within the strain revealed that tubulysin assembly is catalyzed by a molecular "assembly line" consisting of polyketide synthase (PKS) and nonribosomal peptide synthetase (NRPS) multienzymes, and a hybrid PKS-NRPS subunit (Figure 1A) (Sandmann et al., 2004). Although the gene set does not incorporate any obvious functions for carrying out the required postassembly line oxidation and acyl transfer reactions, we identified a gene encoding a lysine cyclodeaminase (*tubZ*), which was assumed to participate in provision of the starter unit pipecolic acid (Khaw et al., 1998; Gatto et al., 2006). To directly probe the function of *tubZ* in An d48, we inactivated the gene by insertional mutagenesis (Ullrich et al., 2009). The resulting mutant, An d48-*tubZ*$^-$, was expected to be deficient in tubulysin

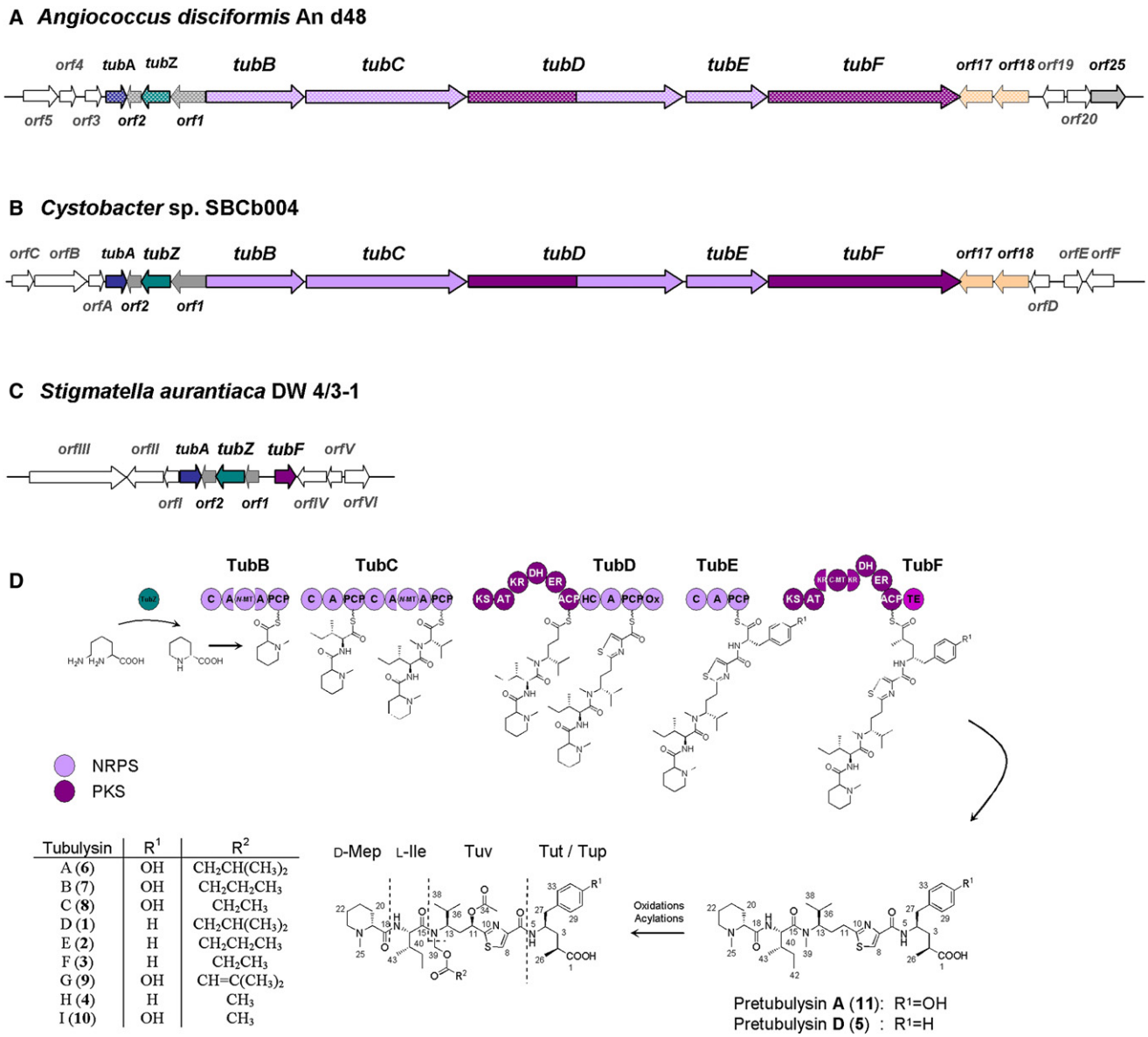

Figure 1. Comparison of Tubulysin Biosynthetic Gene Clusters in An d48 and SBCb004

(A) Genetic organization of the tubulysin gene cluster in *Angiococcus disciformis* An d48. Based upon the newly determined cluster boundaries, we have redesignated gene *tubG* (Sandmann et al., 2004) as *orf25*, reflecting the fact that it is not part of the tubulysin pathway.

(B) Genetic organization of the tubulysin gene cluster in *Cystobacter* sp. SBCb004.

(C) Genetic organization of the tubulysin gene cluster fragment in *Stigmatella aurantiaca* DW 4/3-1.

(D) Model for tubulysin biosynthesis, showing the domain organization of the PKS-NRPS assembly line and the structures of the chain extension intermediates. The structures of the ten known tubulysins (**1**–**10**) are shown, as well as that of the newly discovered compound, pretubulysin A (**11**).

biosynthesis, but instead generated tubulysin D at approximately 3% of wild-type levels. The continued availability of pipecolic acid to the pathway was attributed to the presence of additional, unidentified lysine cyclodeaminase function(s) in *A. disciformis* (Ullrich et al., 2009). In addition, analysis by high-resolution tandem mass spectrometry and comparison with authentic, synthetic standard, showed that An d48-*tubZ*$^-$ appeared to accumulate the presumed first enzyme-free intermediate in the tubulysin pathway, pretubulysin D (**5**). The same metabolite was also detected in the wild-type strain, supporting its intermediacy in the biosynthesis. Although yields of pretubulysin D were insufficient to enable unambiguous confirmation of its structure by nuclear magnetic resonance (NMR), the compound was shown to retain the high tubulin-degrading activity of its more complex tubulysin relatives (Ullrich et al., 2009).

To obtain further insights into tubulysin biosynthesis via comparative cluster analysis, we aimed to identify the gene cluster in a second myxobacterial strain, *Cystobacter* sp. SBCb004 (Figure 1B). In common with *Archangium gephyra* Ar315, *Cystobacter* SBCb004 generates tubulysins A (**6**), B (**7**),

Table 1. Proteins Encoded in the Sequenced Region in the SBCb004 Tubulysin Biosynthetic Gene Cluster and their Putative Functions

NRPS/PKS Portion of the Gene Cluster

Protein	aa	Proposed Function (protein domains with their position in the sequence)[a]
TubB	1520	NRPS domains: C (62–493), A (494–1416), *N*-MT (971–1368), PCP (1432–1500)
TubC	2628	NRPS domains: C (77–515), A (516–1027), PCP (1044–1112), C (1136–1569), A (1570–2499), *N*-MT (2042–2451), PCP (2514–2582)
TubD	3511	PKS domains: KS (11–441), AT (527–852), KR (939–1370), DH (1371–1652), ER (1678–1980), ACP (2062–2157) NRPS domains: HC (2190–2624), A (2625–3138), PCP (3153–3223), Ox (3231–3509)
TubE	1161	NRPS domains: C (47–482), A (483–1034), PCP (1051–1121)
TubF	2843	PKS domains: KS (5–436), AT (522–847), KR (925–1721), *C*-MT (1309–1540), DH (1722–1997), ER (2023–2322), ACP (2404–2506), TE (2541–2815)

ORFs Encoded Upstream and Downstream of *tubB–tubF*

Protein	aa	Proposed Function of the Homologous Protein	Source of the Homologous Protein	Similarity/ Identity	GenBank Accession Number
OrfC	735	Outer membrane protein, OMP85 family, putative	*Stigmatella aurantiaca*	71%/57%	EAU64371.1
OrfB	1549	Hypothetical protein MXAN_6465	*Myxococcus xanthus*	65%/48%	ABF91418.1
OrfA	273	α/β hydrolase fold	*Geobacter uraniireducens*	91%/81%	ABQ27606.1
TubA	432	TubA	*Stigmatella aurantiaca*	89%/81%	EAU66910.1
Orf2	219	Conserved hypothetical protein	*Stigmatella aurantiaca*	86%/74%	EAU66945.1
TubZ	386	TubZ	*Stigmatella aurantiaca*	91%/86%	EAU66930.1
Orf1	394	Hypothetical protein (Orf1)	*Angiococcus disciformis*	90%/78%	CAF05646.1
Orf17	337	Patatin-like protein (Orf18)	*Angiococcus disciformis*	77%/62%	CAF05653.1
Orf18	368	Patatin-like protein (Orf18)	*Angiococcus disciformis*	82%/68%	CAF05653.1
OrfD	124	Chloroplast heat shock protein 70	*Pennisetum glaucum*	50%/33%	ABP65327.1
OrfE	119	ChpK	*Stigmatella aurantiaca*	93%/89%	EAU64035.1
OrfF	271	Protein kinase	*Stigmatella aurantiaca*	49%/33%	EAU63389.1

For the corresponding proteins in *A. disciformis* An d48 gene cluster, please see (Sandmann et al., 2004).
[a] Domain boundaries were assigned, when possible, based on the solved structures of the individual domains.

C (**8**), G (**9**), and I (**10**) (Figure 1D), incorporating tubutyrosine instead of the tubuphenylalanine of tubulysins D, E, F and H. The SBCb004 tubulysin gene cluster closely resembles that in An d48 (compare Figures 1A and 1B), allowing straightforward determination of the cluster boundaries in both myxobacteria. Like its An d48 counterpart, no genes encoding post-PKS tailoring functions were present in the SBCb004 tubulysin cluster. As anticipated, a *tubZ* disruption mutant in SBCb004 accumulated the tubutyrosine analog of pretubulysin D, pretubulysin A (**11**) (Figure 1D). In this case, yields were sufficient to allow verification of the structure for the first time by NMR. In addition, on the basis of NMR, feeding experiments and high-resolution mass spectrometry (MS) analysis, we report the existence of 22 additional novel tubulysin derivatives from both SBCb004 and An d48.

RESULTS AND DISCUSSION

Discovery and Annotation of the Tubulysin Biosynthetic Gene Cluster in *Cystobacter* SBCb004

To locate the tubulysin gene cluster in *Cystobacter* SBCb004, we shot-gun sequenced the genome to 276 contigs using 454 technology (Margulies et al., 2005; Rothberg and Leamon, 2008), and then analyzed the data by BLAST (Altschul et al., 1997) using *tub* genes from An d48 (Sandmann et al., 2004). Genes within an 82 kb region were then functionally annotated. By identification of the gene set common to both SBCb004 and An d48, we were able for the first time to define the cluster boundaries in both organisms. The clusters each incorporate 11 genes, which are present in the same order and orientation (Figures 1A and 1B and Table 1). The core biosynthetic genes (*tubB–tubF*) encode three NRPS subunits, one PKS multienzyme, and a hybrid PKS-NRPS protein. Two conserved open reading frames (orfs) (*orf17* and *orf18*) are present downstream of gene *tubF*, whereas *tubB* is preceded by genes *tubA*, *orf2*, *tubZ,* and *orf1*. Gene *orf1* is predicted to encode an anion-transporting ATPase, whereas the *orf2* gene product exhibits similarity to hypothetical proteins. Mutual sequence homology between the SBCb004 and An d48 proteins is high (Orf1: 78% identity/90% similarity; Orf2: 69% identity/82% similarity versus 68%–73% identity/78%–81% similarity for the PKS/NRPS proteins), which suggests evolutionary pressure to maintain their functions. However, neither Orf1 nor Orf2 has an obvious role to play in tubulysin biosynthesis.

The product of gene *tubA* shows similarity to NRPS C domains (Sandmann et al., 2004). Notably, a sequence (DHxxxDx) within core motif C3 is closely similar to a proposed signature sequence (HHxxxDG) for enzymes that effect acyl transfer, such as chloramphenicol acyltransferase and dihyrolipoamide acyltransferase (De Crecy-Lagard et al., 1995). Thus, TubA may serve

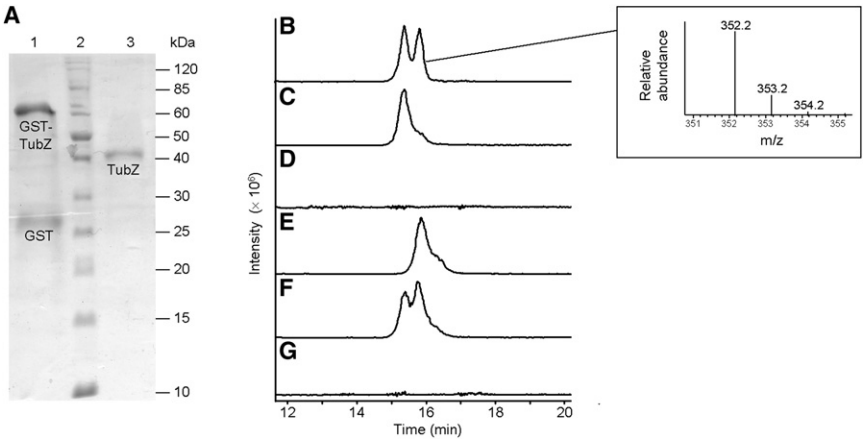

Figure 2. Characterization of TubZ Cyclodeaminase Activity

(A) SDS-PAGE analysis of GST-TubZ (lane 1) and discrete TubZ (lane 3). Lane 2 contains molecular weight markers, with the indicated masses. The calculated molecular weight of GST-TubZ is 67.698 kDa, whereas that of TubZ is 40.501 kDa.

(B) Chiral HPLC-MS analysis (extracted ion chromatogram [EIC], *m/z* $[M+H]^+$ = 352.2) of a 1:1 mixture of Fmoc-derivatized, commercially available L- and D-pipecolic acid. Peak identities were assigned by comparison to analysis of Fmoc-derivatized D-pipecolic acid alone. Inset is the mass spectrum of Fmoc-derivatized L-pipecolic acid (calculated *m/z* $[M+H]^+$ = 352.16).

(C) Chiral HPLC-MS (EIC) analysis of the Fmoc-derivatized commercially available D-pipecolic acid alone.

(D) Chiral HPLC-MS (EIC) analysis of the TubZ reaction carried out in the presence of D-lysine.

(E) Chiral HPLC-MS (EIC) analysis of the TubZ reaction carried out in the presence of L-lysine.

(F) Mixture of the assay shown in (E) and Fmoc-derivatized D-pipecolic acid (C).

(G) Chiral HPLC-MS (EIC) analysis of a representative negative control reaction carried out with L-lysine in the absence of TubZ.

as one of the missing acyl transferases in the tubulysin pathway. In support of a shared role for the TubA proteins in the two strains, the SBCb004 and An d48 homologs show a high degree of sequence conservation (56% identity/73% similarity). However, the proposed functions remain to be directly demonstrated. *orf17* and *orf18* both encode patatin-like proteins, which show high mutual sequence homology (60% identity/70% similarity in the case of the SBCb004 proteins), suggesting evolution by gene duplication. Interestingly, the closest homolog to both Orf17 and Orf18 in SBCb004 is Orf18 of An d48, which may imply that *orf17* of An d48 has diverged from the other sequences. Patatin-like proteins exhibit lipid acyl hydrolase activity (Moraleda-Munoz and Shimkets, 2007; Banerji and Flieger, 2004), a function apparently not required in the tubulysin pathway. Intriguingly, however, genes encoding patatin-like proteins are also present in the DKxanthene gene clusters of the myxobacteria *Myxococcus xanthus* DK1622 and *Stigmatella aurantiaca* DW4/3-1 (Meiser et al., 2008), suggesting that the enzymes may play a previously unsuspected role in natural product biosynthesis.

Predictably from the defined boundaries, orfs upstream of *tubA* and downstream of *orf18* in both organisms have no obvious function in the tubulysin pathway. Thus, the oxidase activities, and possibly a second acyl transferase enzyme in addition to TubA, are apparently lacking in both clusters, and so are presumed to be located elsewhere in the genome. Such split cluster PKS/NRPS architecture is unusual for *Streptomyces*, but has precedent in the myxobacteria (Carvalho et al., 2005; Kopp et al., 2005; Perlova et al., 2006). The fact that this split organization is conserved in two different species argues for the presence of the tubulysin genes in an ancestor common to both *Cystobacter* SBCb004 and *Angiococcus* An d48—that is, that the cluster evolved into its present form prior to the speciation event within the Cystobacterineae suborder. Phylogenetic analysis based on 16S rDNA supports this hypothesis, because An d48 and SBCb004 belong to the same family, sharing membership with another potential tubulysin producing-strain *Archangium gephyra* Ar g1 (see Figure S1 available online).

Analysis by BLAST also revealed a portion of the tubulysin gene cluster comprising *tubA*, *orf2*, *tubZ*, and fragments of *orf1* and *tubF*, in the publically available genome of a third myxobacterial strain, *Stigmatella aurantiaca* DW 4/3-1 (Figure 1C). This architecture may have arisen from deletion of the intervening genes (*tubB–tubE*) from an ancestral cluster. Interestingly, the *Cystobacter* TubA, Orf2, and TubZ proteins show higher sequence identity to their *Stigmatella* homologs than to those of *Angiococcus* (Table 1), despite the closer evolutionary relationship between *Cystobacter* and *Angiococcus* (as judged on the basis of 16S rDNA) (Figure S1). Consistent with the fact that only part of the gene cluster is present in *S. aurantiaca*, the strain is not known to produce any of the tubulysins.

Investigation of the Stereochemistry of the Pipecolic Acid Starter Unit

The final configuration of the *N*-methyl pipecolic acid in the tubulysins is D (Steinmetz et al., 2004), and therefore we hypothesized that free D-pipecolic acid (either generated directly by the cyclodeaminase TubZ, or by epimerization of an initially-formed L-isomer), might be selected as a substrate by the tubulysin PKS-NRPS. Interestingly, the lysine cyclodeaminases RapL from the rapamycin pathway (40% identity/53% similarity to TubZ) and Pip from friulimicin biosynthesis (45% identity/56% similarity to TubZ) have been shown to generate exclusively L-pipecolic acid from L-lysine (Khaw et al., 1998; Gatto et al., 2006; Müller et al., 2007). To address the stereospecificity of TubZ, we expressed the An d48 enzyme in recombinant form as a C-terminal translational fusion with glutathione-*S*-transferase (GST) (see Experimental Procedures), and confirmed the identity of the protein by matrix assisted laser desorption ionization-time-of-flight mass spectrometry (MALDI-TOF-MS) analysis. TubZ was purified as its GST fusion, and also as a discrete protein by on-column cleavage of GST using PreScission Protease® (Figure 2A). The recombinant TubZ proteins (1.5 μM GST-TubZ or 0.6 μM TubZ) were then incubated with either L- or D-lysine (1 mM), NAD^+ (100 μM), and BSA (14 μM) at 30°C for 24 hr (Gatto et al., 2006). The reactions were quenched

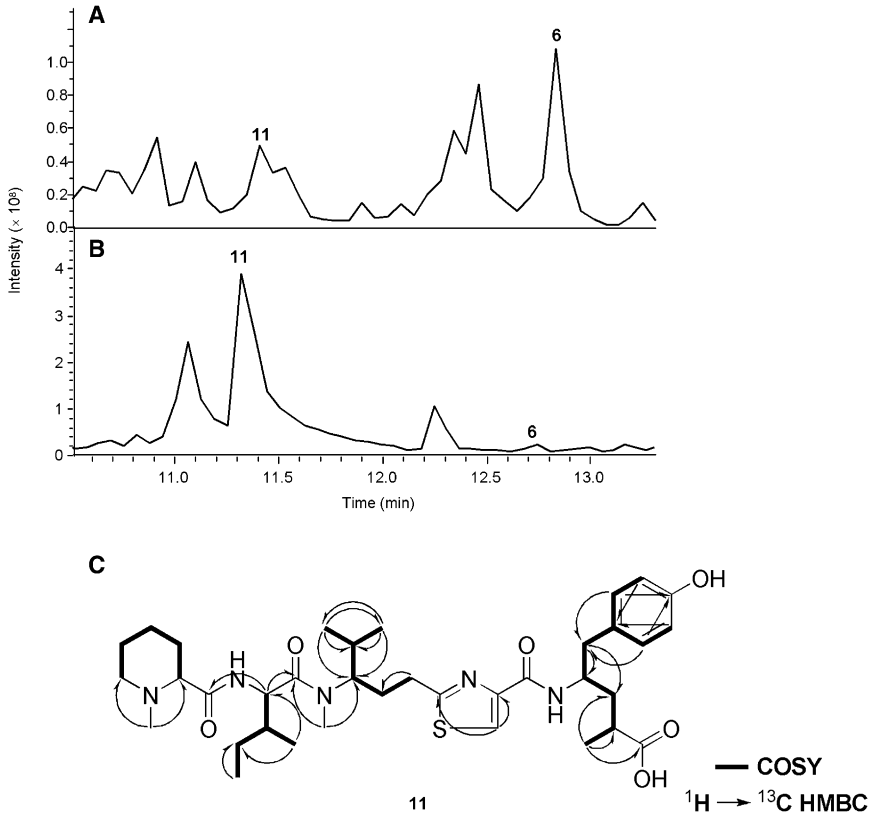

Figure 3. Production of Tubulysin A and Pretubulysin A by SBCb004 Wild-Type and Mutant SBCb004-*tubZ*⁻

(A) HPLC-MS analysis (base peak chromatogram [BPC]) of wild-type SBCb004. Peaks corresponding to tubulysin A (**6**) and pretubulysin A (**11**) are indicated.

(B) HPLC-MS analysis (BPC) of extracts of mutant SBCb004-*tubZ*⁻. Peaks corresponding to tubulysin A (**6**) and pretubulysin A (**11**) are indicated.

(C) [^{1}H, ^{1}H]-COSY (**bold** bonds) and HMBC (arrows) couplings determined for pretubulysin A (**11**). Only a subset of HMBC couplings have been included within the tyrosine aromatic ring.

by the addition of acetonitrile. Prior to analysis by high-performance liquid chromatography-mass spectrometry (HPLC-MS), the assay mixtures were derivatized with 9-fluorenylmethyl chloroformate (Fmoc-Cl). Crucially, we were able to separate Fmoc-derivatized, commercially available L- and D-pipecolic acid from each other by chiral chromatography (Figures 2B and C). Assays with the lysine substrates and GST-TubZ or discrete TubZ gave identical results. In each case, analysis of the assay containing D-lysine did not reveal any evidence for formation of the product pipecolic acid (Figure 2D), relative to controls performed with L-/D-lysine in the absence of TubZ (Figure 2G). In contrast, pipecolic acid was detected in the assays with L-lysine (Figure 2E), and was shown to be exclusively the L-isomer by spiking the assay mixture with authentic, derivatized D-pipecolic acid (Figure 2F). Thus, TubZ shows the same substrate and product stereospecificities as RapL and Pip.

At this stage, it remained a possibility that the L-pipecolic acid generated by TubZ was epimerized to the D-isomer before activation by TubB by an as yet unidentified epimerase. To probe this question directly, we synthesized both enantiomers of pipecolic acid in 4,5-di-deuterium-labeled form via ring closing metathesis (Grubbs et al., 1995; Schuster and Blechert, 1997) of an *N*-allylated γ,δ-unsaturated amino acid, followed by catalytic deuteration (Schneider and Kazmaier, 1998; Kazmaier and Schneider, 1998; Zumpe and Kazmaier, 1998, 1999; Miller et al., 1998). The enantiomerically pure materials were then administered to cultures of both wild-type An d48 and the An d48-*tubZ*⁻ mutant (Ullrich et al., 2009). Analysis by HPLC-MS (Figure S2) showed that only the L-isomer of pipecolate was incorporated in either case, strongly suggesting that epimerization occurs following attachment of the amino acid to the multienzyme. However, module TubB (Figure 1) lacks a classical epimerization (E) domain (Luo et al., 2002; Stachelhaus and Walsh, 2000) to generate the required stereochemistry. Further support for the lack of epimerization by TubB comes from phylogenetic analysis of the TubC condensation domain that accepts the *N*-methyl pipecolic acid as substrate: the C domain clusters together with other C domains with demonstrated specificity for L-amino acids at both their donor and acceptor sites (so-called $^{L}C_{L}$ domains) (Rausch et al., 2007) (Figure S3). This analysis also argues against the possibility that the TubC C domain functions as a condensase/epimerase (Balibar et al., 2005), a dual-function domain that has been shown in other NRPS pathways to convert L-amino acids to their D-isomers. Thus, epimerization apparently occurs downstream of the first round of chain extension and is likely to be catalyzed by an external racemase (Dubern et al., 2008). Intriguingly, only the PCP domain of TubD incorporates a sequence motif at the phosphopantetheine attachment site (GXDSX), which resembles the GGDSI motif previously implicated in recognition between E and PCP domains in *cis* (Linne et al., 2001), perhaps indicating that the epimerization in *trans* may occur at this stage of chain extension. However, further studies will be required to elucidate the precise timing of this cryptic reaction.

Generation of a *tubZ* Mutant of SBCb004 to Enable Structure Elucidation of Pretubulysin A

Although analysis by mass spectrometry of pretubulysin D (**5**) from An d48 strongly supported its proposed structure (Ullrich et al., 2009), we aimed to obtain sufficient quantities of its pretubulysin A analog to allow structural proof by NMR. A compound with a mass (*m/z* 686.4 $[M+H]^+$) consistent with pretubulysin A (**11**) was identified in extracts of the *Cystobacter* sp. SBCb004 wild-type strain, at 42% yield relative to tubulysin A (**6**) (Figure 3A). Because we had previously observed that the An d48-*tubZ*⁻ mutant produced increased amounts of pretubulysin D relative to wild-type *A. disciformis* (Ullrich et al., 2009), we

hoped to boost the titer of pretubulysin A in SBCb004 by engineering the equivalent *tubZ* mutation (Figure S4). HPLC-MS analysis of the resulting mutant, SBCb004-*tubZ*$^-$, revealed that the strain accumulated pretubulysin A at approximately 5-fold wild-type levels, whereas the production of tubulysin A was decreased by 20-fold (Figure 3B). The availability of the genome sequence of SBCb004 allowed us to probe for the presence of additional lysine cyclodeaminases in the strain, which could complement the inactivated TubZ. BLAST analysis revealed two genes with homology to ornithine cyclodeaminases (20% and 25% sequence identity to TubZ). Because RapL exhibits ornithine cyclodeaminase activity as a side reaction (Gatto et al., 2006), it seems reasonable that the detected ornithine cyclodeaminases may catalyze low levels of lysine cyclodeamination, explaining the continued presence of pipecolic acid in the SBCb004-*tubZ*$^-$ mutant. Given the evolutionary relationship between *Cystobacter* SBCb004 and *Angiococcus disciformis* An d48 (Figure S1), it is likely that An d48 harbors homologs of these two genes.

Purification of Pretubulysin A and NMR Structure Elucidation

To generate enough pretubulysin A to enable purification, SBCb004-*tubZ*$^-$ was grown on the 26 L scale in the presence of XAD adsorber resin. Pretubulysin A was then purified from a methanolic resin extract by silica gel chromatography, followed by preparative HPLC, yielding 6.5 mg material. High-resolution electrospray ionization mass spectrometry (HR-ESI-MS) revealed a monoisotopic mass (*m/z* $[M+H]^+$ = 686.3941 Da) corresponding, as predicted, to a molecular formula of $C_{36}H_{56}N_5O_6S$. Structure elucidation was accomplished using combined one- and two-dimensional (1D and 2D) NMR experiments (^1H, ^{13}C, [^1H, ^1H]-COSY, [^1H, ^{13}C]-HSQC, and [^1H, ^{13}C]-HMBC) (Figure S5). As the interpretation of the NMR spectra of the tubulysins is complicated by missing and overlapping signals (Steinmetz et al., 2004), reference spectra of synthetic pretubulysin D (**5**) (Ullrich et al., 2009) were recorded in the same solvent and on the same instrument, in order to allow for direct comparison of the data (Table 2).

This approach enabled the assignment of the majority of pretubulysin A signals, which were in good agreement with those observed from synthetic pretubulysin D. The exceptions (19-H, 23-H and 25-H) are likely due to the fact that pretubulysin A was only partially protonated at N24 under the purification conditions, while pretubulysin D was analyzed as its trifluoroacetic acid (TFA) salt, which likely resulted in a higher degree of protonation at this position (Steinmetz et al., 2004). Pretubulysin A signals that could not be assigned with confidence from the ^1H NMR spectrum included most of the methylene groups, the proton at C13, and the protons within the piperidine ring of pipecolic acid (Figure 1D). The exact chemical shifts for all of these protons were therefore deduced from [^1H,^1H]-COSY data. The COSY couplings were also used to verify the structures of the individual building blocks in the molecule, Mep, Ile, Tuv, and Tut (Figure 1D). All carbon signals with the exception of the C6 carbonyl were assigned for the biosynthetic compound by [^1H, ^{13}C]-HSQC, and [^1H, ^{13}C]-HMBC, and showed good agreement with the corresponding data for the synthetic material. Even with 24 mg synthetic pretubulysin D, the C6 carbonyl signal was barely visible in the ^{13}C NMR spectrum, and therefore the 6.5 mg purified pretubulysin A was insufficient to assign this peak. We also confirmed the correct sequence of building blocks from the [^1H, ^{13}C]-HMBC connectivities (Figure 3C). The only connection which could not be established in this way was that between tubuvaline and tubutyrosine, due to the absence of a signal for the C6 carbonyl (this connectivity was also missing in the HMBC of synthetic pretubulysin D). Nonetheless, taken together, the combined data from the 1D and 2D NMR experiments strongly support our proposed structure for pretubulysin A.

Analysis of the Two Strains for Novel Metabolites

The presence of the pretubulysins in the wild-type strains prompted us to reanalyze the extracts for additional metabolites, which may have escaped detection in earlier experiments. In fact, we found 11 further candidates for novel compounds in *A. disciformis* An d48, with molecular masses *m/z* $[M+H]^+$ = 628.4, 656.4, 670.4 (different retention time than that of pretubulysin D), 672.4, 686.4 (× 2), 700.4, 714.4, 744.4, 772.4, and 786.4 (Figure 4). Although most of these metabolites appeared to be minor in comparison with tubulysin D (see Figure 4 for yield estimates), compound 670.4 was present in significant amounts (as judged by relative peak area in the HPLC-MS chromatogram). In each case, a likely relationship to the tubulysins was established by feeding deuterium-labeled L-pipecolic acid, valine, or both and by comparison of the incorporation pattern to that of pretubulysin D (**5**) (Figure S2). Comparison of the fragmentation patterns of metabolites 772.4 and 786.4 with those of the tubulysins D–F and H (Figure S6) allowed us to assign the structures to desacetyl tubulysin E (**12**) and desacetyl tubulysin D (**13**), respectively (Figure 4). Although biosynthetic considerations (i.e., the defined stereospecificities of adenylation (A) and *C*-methyltransferase (MT) domains) strongly suggest that the stereochemistry of these metabolites should be shared with the parent compounds, we cannot make any definitive statements on this issue in the absence of NMR data.

We next obtained compound 670.4 at high purity (1.3 mg), and determined its accurate mass. The most probable molecular formula, $C_{35}H_{51}N_5O_6S$, differs from pretubulysin D by $-CH_4$ and +O, demonstrating that the new compound is not simply a stereoisomer of pretubulysin D. We hypothesized that the metabolite might have lost a methyl group relative to pretubulysin D (accounting for $-CH_2$), and that it would incorporate an extra oxygen (+O) and a site of unsaturation (–2H) (e.g., a carbonyl functionality). To confirm these expectations, cultures of wild-type *A. disciformis* were grown in the presence of d_3-methionine, in order to generate a pool of [methyl-d_3]-*S*-adenosylmethionine ([methyl-d_3]-SAM) in the cell. Analysis of the resulting extracts showed that while tubulysin D incorporated three SAM-derived methyl groups (maximum mass shift of +8), compound 670.4 contained only two (+6) (compare Figures 5A and 5B). To determine the location of the missing methyl group, we elucidated the fragmentation pattern of 670.4 by comparison to that of pretubulysin D (Figure S7). This analysis revealed that deuterium labeling occurred exclusively on the *N*-methyl of pipecolic acid, and/or the methyl of tubuphenylalanine (Figure 5C). We therefore concluded that compound 670.4 lacks the *N*-methyl group of valine. Further support for this hypothesis

Table 2. Comparison of ^{1}H NMR (500 MHz, CD_3OD), ^{13}C NMR (125 MHz, CD_3OD) and 2D NMR (HSQC, HMBC) Spectroscopic Assignments of Synthetic Pretubulysin D and Biosynthetic Pretubulysin A

		Synthetic Pretubulysin D[a]			Isolated Pretubulysin A		
Position (C)	Position (H)	δ_C (ppm)	δ_H (ppm) (m, *J* [Hz])	HMBC (^{1}H to ^{13}C)	δ_C (ppm)	δ_H (ppm) (m, *J* [Hz])	HMBC ($^{1}H \rightarrow ^{13}C$)
1		180.2			180.3		
2	2-H	37.4	2.55 (m)		38.0	2.55 (m)	
3	3a-H	39.0	1.71 (m)		39.1	1.68 (m)	
	3b-H		2.01 (m)			2.01 (m)	
4	4-H	50.4	4.36 (m)		50.8	4.30 (m)	
6		163.2			-		
7		150.7			150.5		
8	8-H	123.7	7.96 (s)	7, 10	123.8	7.96 (s)	7, 10
10		172.0			171.7		
11	11a-H	30.8	2.86 (m)		30.8	2.85 (m)	12
	11b-H		2.95 (m)			2.95 (m)	12
12	12a-H	30.0	1.99 (m)		30.0	1.99 (m)	
	12b-H		2.18 (m)			2.17 (m)	
13	13-H	60.3	4.37 (m)		60.4	4.33 (m)	
15		174.7			174.5		
16	16-H	55.7	4.70 (d, 8.3)	15, 18, 40, 41	55.6	4.73 (d, 8.4)	15, 18
18		169.4			170.2		
19	19-H	67.8	3.77 (dd, 12.0, 2.8)		68.3	3.58 (m)	
20	20a-H	29.9	1.80 (m)		30.1	1.78 (m)	
	20b-H		2.15 (m)			2.06 (m)	
21	21-H	22.3	1.60 (m)		22.4	1.54 (m)	
22	22a-H	23.6	1.78 (m)		24.2	1.76 (m)	
	22b-H		1.92 (m)			1.85 (m)	
23	23a-H	56.0	3.07 (brs)		56.2	2.85 (m)	
	23b-H		3.49 (d, 12.3 Hz)			3.40 (brs)	
25	25-H_3	42.6	2.74 (s)	19, 23	43.2	2.63 (s)	19, 23
26	26-H_3	18.2	1.16 (d, 7.2)	1, 2, 3	18.3	1.16 (d, 7.2)	1, 2, 3
27	27-H	42.0	2.89 (m)	3, 4, 28, 29, 33	41.2	2.81 (m)	3, 4
28		139.7			130.3		
29	29-H	130.6	7.22 (m)	27, 28	131.3	7.03 (d, 8.3)	27,30, 31, 32, 33
30	30-H	129.5	7.22 (m)	27, 28	116.2	6.68 (m)	28, 31, 32
31		127.6	7.15 (m)	30, 32	156.8		
32	32-H	129.5	7.22 (m)	27, 28	116.2	6.68 (m)	28, 30, 31
33	33-H	130.6	7.22 (m)	27, 28	131.3	7.03 (d, 8.3)	27, 29, 30, 31, 32
36	36-H	31.2	1.80 (m)		31.2	1.80 (m)	
37	37-H_3	20.0	0.80 (d, 6.5)	13, 36, 38	20.1	0.79 (d, 6.5)	13, 36, 38
38	38-H_3	20.3	0.98 (d, 6.5)	13, 36, 38	20.2	0.97 (d, 6.5)	13, 36, 37
39	39-H_3	30.1	3.10 (s)	13, 15	30.4	3.07 (s)	13, 15
40	40-H	37.2	1.92 (m)		37.6	1.92 (m)	
41	41a-H	25.3	1.24 (m)		25.3	1.23 (m)	
	41b-H		1.61 (m)			1.61 (m)	
42	42-H_3	11.0	0.92 (t, 7.4)	40, 41	11.1	0.90 (t, 7.4)	41
43	43-H_3	15.8	1.02 (d, 6.8)	16, 40, 41	15.9	1.00 (d, 6.8)	16, 41

[a] Pretubulysin D was analyzed as its trifluoroacetic acid (TFA) salt.

was obtained by NMR analysis. The ^{1}H NMR spectra of pretubulysins D (**5**) and A (**11**) (Figure S5) exhibit two clear singlet signals corresponding to the *N*-methyl groups (Table 2 and Figure 5D), with the C39 *N*-methyl signal (Figure 1) appearing downfield of the C25 methyl (δ 3.07 and 2.63 ppm respectively, for pretubulysin A). Inspection of the spectrum of metabolite **14** (Figures 5E

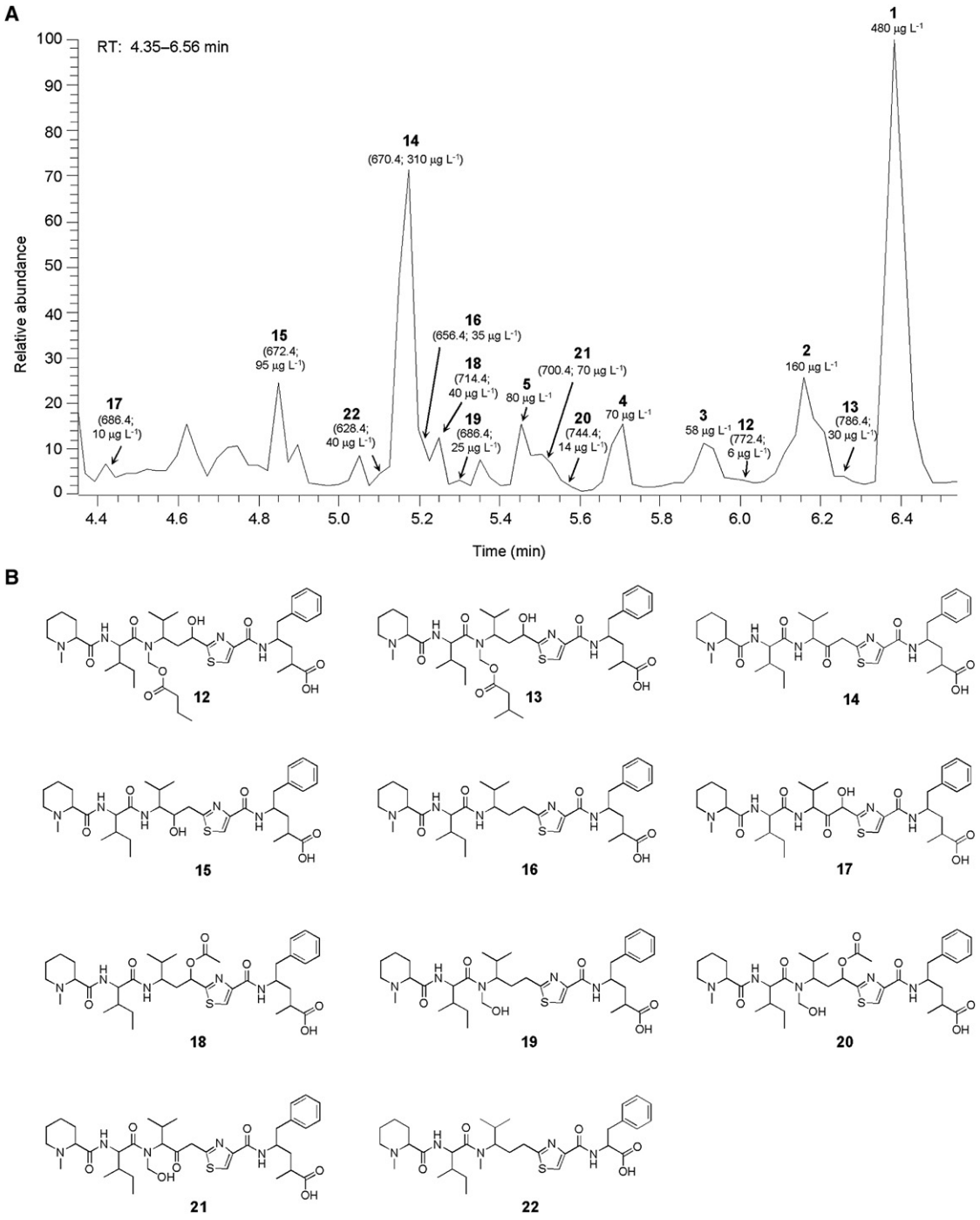

Figure 4. Novel Tubulysins Produced by *A. disciformis* An d48

(A) HPLC-MS analysis (BPC) of wild-type extracts. Peaks corresponding to the five known (**1**–**5**) and eleven novel tubulysins (**12**–**22**) are indicated.
(B) Proposed structures of compounds **12**–**22**.

and S5) reveals a single *N*-methyl signal, which on the basis of its chemical shift (δ 2.35 ppm), can be assigned to the C25 methyl. To account for the introduction of a carbonyl group, we considered a biosynthetic mechanism in which an oxygen atom which is normally lost could be retained in the structure. This focused attention on the two PKS modules which normally process the β-carbonyl of the chain extension intermediate to a methylene, and the respective carbons, C3 and C12. Based on the appearance of new fragment peaks at mass 361.1 and 343.1 Da, corresponding to cleavage adjacent to C12 (Figure S6), we identified this carbon as the most probable site of modification. Thus, 670.4 is proposed to be *N*-desmethyl 12-keto pretubulysin D (**14**).

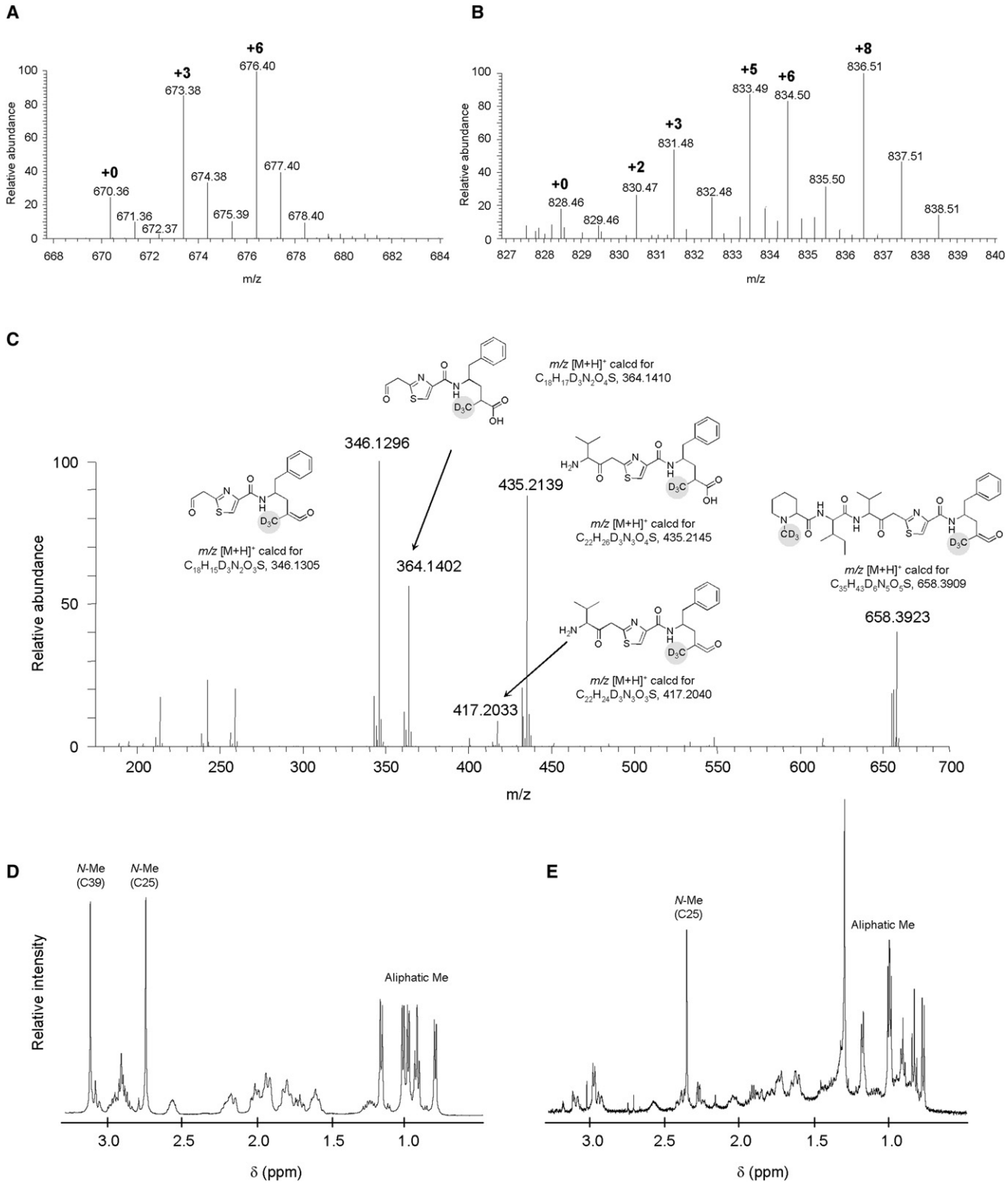

Figure 5. Identification of *N*-Desmethyl 12-keto Pretubulysin (14)

(A) High-resolution MS analysis of 14 from cultures supplemented with d_3-methionine. Labeling occurred at either or both of the C25 and C26 methyl groups, generating mass shifts of +3 and +6, respectively.

(B) High-resolution MS analysis of tubulysin D (**1**) from cultures supplemented with d_3-methionine. Labeling occurred at either or both of the C25 and C26 methyl groups and/or at the C39 methylene, giving rise to the characteristic +2, +3, +5, +6, and +8 labeling pattern.

With this structure in hand, it was possible to assign compounds 656.4 and 672.4, to *N*-desmethyl pretubulysin analogs in which the C12 carbonyl group had alternately been reduced to a hydroxyl (672.4; *N*-desmethyl 12-hydroxy pretubulysin D (**15**)), or to a methylene functionality (656.4; *N*-desmethyl pretubulysin D (**16**)) (Figure 4; Figures S6 and S7); in the case of compound **15**, however, we cannot rule out the alternative that the hydroxyl group is instead located at the adjacent C11 position, consistent with post-assembly line hydroxylation of metabolite **16**. In any case, a compound corresponding to the intermediate dehydrated analog was not detected. In addition, one of the two compounds with mass *m/z* $[M+H]^+$ = 686.4 (**17**) appears to be the 11-hydroxy version of metabolite **14**. By MS analysis, it was also possible to putatively identify compound 714.4 as *N*-desmethyl 11-acetoxy pretubulysin D (**18**) (Figure 4; Figures S6 and S7), referred to in earlier synthesis literature as tubulysin U (Dömling et al., 2006; Sani et al., 2007; Balasubramanian et al., 2009), demonstrating that at least two of the normal post-assembly line modifications can occur even in the absence of *N*-methylation. By similar logic, the second peak at 686.4 was attributed to *N*-hydroxymethyl pretubulysin (**19**) and that at 744.4 to its 11-acetoxy analog (**20**) (Figure 4; Figures S6 and S7). Analysis of the compound 700.4 revealed fragments consistent with the presence of an *N*-hydroxymethyl functionality and a 12-keto group, leading to its identification as *N*-hydroxymethyl 12-keto pretubulysin D (**21**). Finally, metabolite 628.4 appears to comprise a truncated pretubulysin derivative in which tubuphenylalanine has been replaced by phenylalanine (**22**) (Figure 4; Figures S6 and S7). As further support for these assignments, incubation in the presence of d_3-methionine revealed the incorporation of two or three labeled methyl groups, as appropriate, into metabolites **5**, **14**–**16**, **18**, **20**–**22** (Figure S2). We next analyzed extracts of wild-type SBCb004 for the corresponding novel tubulysins, using the same analytical methodology. This comparison revealed a tubutyrosine analog for each of the new compounds (compounds **23**–**33**) (Table S1 and Figure S8). As with the tubulysin D series, the amounts of these compounds relative to tubulysin A were uniformly low; however the specific yield profiles for the various analogs differ between the strains.

Although the amounts of the new metabolites enabled structure elucidation by mass spectrometry, the yields were insufficient to allow full structure proof by NMR, or evaluation of cytotoxicity relative to the parent compounds. Nonetheless, the high-resolution MS analysis of the parent ions and all fragments is fully consistent with the suggested structures, there is strong internal concordance among the proposed fragmentation patterns (Figure S6), and the structural assignments are in complete agreement with the feeding studies. In further support of our MS-based methodology, the structure hypothesized for pretubulysin on the basis of the MS data (Ullrich et al., 2009) was subsequently shown to be correct by NMR, and all available NMR evidence suggests that the structure of *N*-desmethyl 12-keto pretubulysin D was also correctly elucidated by MS analysis. In addition, the mode of biosynthesis significantly restricts the number of possible structures (including stereochemistry) that can result from the tubulysin pathway. Importantly, in every case, our proposed structures can be rationalized in terms of reasonable variations in the action of a specific domain or domains within the assembly lines.

Conclusions

The identification of 23 novel tubulysins in *A. disciformis* and *Cystobacter* reveals new aspects of the biosynthesis, and supports earlier proposals. For example, our results strongly suggest that pretubulysin D/A (**5**, **11**) are the products of the hybrid PKS-NRPS in each strain. More generally, our data show that several steps in the pathway do not go to completion. The presence in the extracts of pretubulysins, and compounds **12**, **13**, **19**, **20** and **23**, **24**, **30**, **31** missing one or more of the oxidation and acylation reactions, demonstrates that post-assembly line modification is relatively inefficient, even in the wild-type strains. This observation is consistent with the absence of obvious tailoring genes (oxidases and perhaps an acyltransferase) within the clusters, arguing for a lack of coevolution of this portion of the pathways. The *N*-methyltransferase domain of subunit TubC also operates only imperfectly—in fact, the *N*-desmethyl compounds (**14**–**18**) and (**25**–**29**) constitute major metabolites of the strain. Apparently, the lack of *N*-methylation somehow induces skipping of some, if not all of the reductive steps carried out by the adjacent PKS module. However, these activities do occasionally function, because the corresponding hydroxyl (**15**, **26**) and methylene (**16**, **27**) analogs are produced at low levels. Processing by post-assembly line enzymes at C11 can also occur, and is more efficient when full reduction has taken place at the adjacent C12 position. This mechanism is inconsistent, however, with the discovery in extracts of *N*-hydroxymethyl 12-keto pretubulysins (**21**, **32**), because the reductive steps have been bypassed even though the *N*-methyl group was added. One possible explanation is that, in a small number of cases, the *N*-methyl is hydroxylated while the intermediate is attached to the assembly line, and this modification also disrupts reductive processing by the PKS module. Finally, the truncated analogs (**22**, **33**) appear to arise from failure of the final chain extension step with malonate, catalyzed by TubF. At this stage it is not clear whether premature release from the assembly line is spontaneous due to stalling of the intermediate at the TubE/TubF interface, or alternatively enzyme-catalyzed, for example by the TE domain, as demonstrated in pikromycin biosynthesis (Kittendorf et al., 2007).

It is intriguing to consider whether the apparent ''failure'' of various enzymes in the tubulysin pathway is in fact favored by evolution to increase the diversity of structures generated by the strain, a proposal known as the ''screening hypothesis'' (Firn and Jones, 2003). Indeed, the production of sometimes large families of metabolites that differ in their core structures appears to be a general feature of myxobacterial secondary metabolism, in which post-assembly line processing is relatively minimal (Weissman and Müller, 2008). However, relevant information on the biological roles of the various tubulysins for the producing organisms is lacking at present. Clearly, though, the PKS-NRPS can process

(C) Determination of the location of the methyl groups in **14**, based upon analysis of deuterium-labeled fragments (compare to Figures S6 and S7).
(D) Portion of the ^{1}H NMR spectrum of pretubulysin D (**5**). Signals arising from aliphatic and *N*-methyl groups are indicated.
(E) Portion of the ^{1}H NMR spectrum of *N*-desmethyl 12-keto pretubulysin (**14**). Comparison with (D) shows that the metabolite is lacking the C39 *N*-methyl group.

a range of structurally divergent intermediates, encouraging the view that the assembly line could be tailored by genetic engineering to produce further variants. Similar observations have been made for the epothilone assembly line, from which multiple epothilone derivatives have been generated by directed modification (Altmann et al., 2009). In the meantime, the novel analogs can be targeted for total synthesis, in order to obtain sufficient materials to extend the ongoing structure-activity studies of the tubulysin metabolites. It is already promising that pretubulysin D (**5**) exhibits activity similar to that of tubulysin A.

SIGNIFICANCE

Small molecules that interact with the eukaryotic cytoskeleton are promising candidates for development as novel antineoplastic agents. This fact explains the significant interest in the tubulysin family of natural products, tubulin modifiers that are active in the low picomolar range against a range of cancer cell lines. Until 2009, nine tubulysins were known from the myxobacterial strains *Angiococcus disciformis* An d48 and *Archangium gephyra* Ar 315. We expanded this family recently with the discovery in *A. disciformis* of pretubulysin D, the presumed first enzyme-free intermediate in the tubulysin pathway. We now report that A. *disciformis* and a third myxobacterial strain *Cystobacter* sp. SBCb004 together produce a further 23 novel tubulysins. Analysis of the molecular basis for this diversity-oriented biosynthesis provides new insights into the function of polyketide synthase (PKS) and non-ribosomal peptide synthetase (NRPS) natural product "assembly lines." We have also shown that pretubulysin D retains much of the potency of its more structurally elaborate relatives. Thus, the 23 additional simplified analogs are attractive targets for chemical synthesis, with the aim of deepening our understanding of structure-activity relationships within the tubulysin family of compounds.

EXPERIMENTAL PROCEDURES

Culture Conditions

Cystobacter SBCb004 was cultivated at 30°C and 170 rpm in M-medium (1% papaic digest of soybean meal, 1% maltose, 0.1% $CaCl_2 \cdot 2H_2O$, 0.1% $MgSO_4 \cdot 7H_2O$, 8 mg/l NaFe-EDTA, 1.19% HEPES, adjusted to pH 7.2 with 10 N KOH). Mutant SBCb004-*tubZ*$^-$ was grown in the presence of kanamycin (100 μg/ml). For analysis of secondary metabolite production, the wild-type and mutant strains were grown at 30°C for 5–7 days in 50 ml M-medium containing 1% adsorber resin Amberlite XAD-16. The resin was separated from the medium by sieving, and then extracted with 40 ml of methanol. The extracts were evaporated to dryness and resuspended in 1 ml methanol before analysis by mass spectrometry. The cultivation and extraction conditions of An d48 wild-type and mutant An d48-*tubZ*$^-$ were as reported earlier (Ullrich et al., 2009).

Inactivation of *tubZ* in SBCb004

The construction of gene $tubZ_{SBCb004}$ knockout in SBCb004 was accomplished by homologous recombination in the encoding regions. Primer pairs, Cbt-Z1 (5′-GAAGTGACTCATGTTGAGCACGAGGGTG-3′) and Cbt-Z2 (5′-GAGCGCACCAGCTCGAAGAG-3′), were designed to amplify the knockout region (864 bp) in the middle of target gene $tubZ_{SBCb004}$, and introduce a stop codon. The amplified DNA fragment was then cloned into pCR 2.1-TOPO vector (Invitrogen) to obtain the inactivation vector pTOPO-tubZ. The $tubZ_{SBCb004}$ inactivation mutant SBCb004-*tubZ*$^-$ was generated by electroporation, as follows: SBCb004 wild-type cells were grown to an OD_{600} 0.8–1.0, and cells were harvested from 2 ml culture by centrifugation at room temperature. The cell pellet was then washed twice with an equal amount of washing buffer (5 mM HEPES [pH 7.2], 0.5 mM $CaCl_2$), and resuspended in 50 μl ddH_2O. Plasmid pTOPO-tubZ (1–3 μg) was then introduced into the cell suspension, and the mixture was electroporated in a 0.1 cm cuvette (200 Ω, 25 mF, and 0.9 kV/cm). M-medium (1 ml) was added to the cells. The suspension was transferred into a 2 ml centrifuge tube and cultivated for 2 hr at 30°C and 800 rpm on a thermomixer. The cells were then mixed with 1 ml M-medium, and plated on M-agar (M-medium with 1.5% agar) containing kanamycin (100 μg/ml). The plates were incubated at 30°C for 1–2 weeks until colonies became visible. Correct integration of plasmid pTOPO–tubZ into the chromosome of SBCb004 was confirmed using three different PCR reactions with primers pTOPO-In (5′-CCTCTAGATGCATGCTCGAGC-3′), pTOPO-Out (5′-TTGGTACCGAGCTCGGATCC-3′), primer A (5′-GTCGGCGAGGGATCACTCGCGGGCTGC-3′; binding in gene *orf2*) and primer B (5′-TGCCTGAAAGAAGGGTTACCGC-3′; binding in gene *orf1*).

Chromatography and Mass Spectrometry

Standard analysis of crude extracts was performed on an HPLC-DAD system from the Agilent 1100 series, coupled to a Brucker Daltonics HCTultra ESI-MS ion trap instrument operating in positive ionization mode. Compounds were separated on a Luna RP-C_{18} column (125 × 2 mm; 2.5 μm particle diameter; flow rate 0.4 ml/min, Phenomenex), with a mobile phase of water/acetonitrile each containing 0.1% formic acid, using a gradient from 5%–95% acetonitrile over 20 min. Detection was by both diode array and ESI-MS. High-resolution mass spectrometry was performed on an Accela UPLC-system (Thermo-Fisher) coupled to a linear trap-FT-Orbitrap combination (LTQ-Orbitrap), operating in positive ionization mode. Separation was achieved using a BEH RP-C_{18} column (50 × 2 mm; 1.7 μm particle diameter; flow rate 0.6 ml/min, Waters), with a mobile phase of water/acetonitrile each containing 0.1% formic acid, using a gradient from 5%–95% acetonitrile over 9 min. The UPLC-system was coupled to the LTQ-Orbitrap by a Triversa Nanomate (Advion), a chip-based nano-ESI interface. In certain experiments, the extracts were fractionated, and single fractions were analyzed by direct infusion. The yield of tubulysin D (Figure 4) was determined from the peak area (base peak chromatogram) by reference to a standard curve generated with authentic, synthetic material (a kind gift of H. Steinmetz). Estimates of the yields of all other metabolites were obtained by comparison of the peak areas to those of tubulysin D.

Cloning, Expression, and Purification of TubZ

The *tubZ* gene was amplified from cosmid F5 (Sandmann et al., 2004) containing the *Angiococcus disciformis* An d48 tubulysin gene cluster (primer pair: 5′-GGAGCCGAATTCGTGAATGCAGTG-3′ (f) and 5′-GGCGGCCGCTACGGCTGGGGC-3′ (r)), introducing flanking EcoRI and *Not*I sites. The resulting product was then ligated with *Eco*RI and *Not*I, and ligated into pGEX-6P-1, previously digested with both *Eco*RI and *Not*I. The fidelity of the PCR reaction was then confirmed by sequencing. The resulting expression construct pGEX-6P-1-TubZ was transformed into *E. coli* strain BL21(DE3)pLyS. The cells were grown in LB medium (1 l) containing ampicillin (100 mg/ml) at 30°C until an OD_{600} of 0.6–0.7 was reached, and then expression was induced by addition of 0.1 mM IPTG. The cultivation was continued at 16°C overnight, and then the cells were harvested by centrifugation. The cell pellets were resuspended in ice-cold lysis buffer (25 ml; 1 × PBS buffer [10 mM Na_2HPO_4, 1.8 mM KH_2PO_4 (pH 7.3), 140 mM NaCl, 2.7 mM KCl], containing 5 mM DTT and 0.5% Triton X-100) and lysed by French Press. The lysis solution was centrifuged (14,000 *g*) at 4°C for 30 min, and then the clarified lysate was mixed with a 50% slurry of glutathione Sepharose 4B beads (2 ml; GE Healthcare), and incubated at room temperature for 30 min, with gentle agitation. The beads were then washed with buffer (1 × PBS buffer; 10 column volumes). In the case of the GST-TubZ fusion protein, elution was performed directly with elution buffer (50 mM Tris-HCl [pH 8.0], 10 mM reduced glutathione); the protein was eluted in three fractions (10 min incubation). Discrete TubZ was obtained by on-column digestion of the bound GST-TubZ fusion protein. For this, PreScission Protease® (5 units) was added to the beads in protease buffer (50 mM Tris-HCl [pH 7.0], 150 mM NaCl, 1 mM EDTA, 1 mM DTT), and incubated at 4°C overnight. The purified proteins were flash frozen in liquid nitrogen, and stored at −80°C until use.

Characterization of TubZ Cyclodeaminase Activity

Assays contained TubZ–GST fusion protein (1.5 μM) or discrete TubZ protein (0.6 μM), L- or D-lysine (1 mM), NAD^+ (100 μM), and BSA (1 mg/ml) were performed in buffer (5 mM Tris-HCl [pH 8]) in a total volume of 100 μl. Control incubations were performed with L- or D-lysine in the absence of added TubZ. After 24 hr incubation at room temperature, the reactions were quenched by the addition of acetonitrile (200 μl). The assay mixture was chilled at −20°C for at least 10 min, and then centrifuged (16,060 *g*) at 4°C for 10 min. Derivatization was carried out on the assay supernatant (240 μl), using Fmoc-Cl (10 mM; 20 μl) in borate buffer (10 mM; 80 μl). The reaction mixture was incubated at room temperature for 30 min, and then quenched by addition of 2 volumes of pure acetic acid. The same derivatization procedure was performed on a commercially available racemic mixture of L-/D-pipecolic acid, and enantiomerically pure D-pipecolic acid. Following centrifugation, the supernatants were analyzed using the HPLC-DAD system (see above) at 25°C. A Nucleodex β-OH column (200 × 4 mm) (Machery-Nagel) was employed for separation with a solvent system consisting of H_2O and acetonitrile, each containing 0.1% formic acid. The following gradient was applied: 30%–95% acetonitrile over 35 min, at a flow rate 0.5 ml/min.

Feeding Studies

Feeding studies of An d48 wild-type and An d48-*tubZ*$^-$ mutant were performed in 50 ml M7 culture (0.5% probion, 0.1% $CaCl_2 \cdot 2H_2O$, 0.1% $MgSO_4 \cdot 7H_2O$, 0.1% yeast extract, 0.5% soluble starch, 1% HEPES [pH 7.4]), with synthetic deuterium-labeled D-/L-pipecolic acid (1 mg), d_8 L-valine (2.5 mg) and d_3 L-methionine (25 mg). The compounds were dissolved in water, sterile filtered and administered in three portions to one-day old cultures in three parts (100 μl every 12 hr). The cells were cultivated for an additional day. 1% Amberlite XAD absorber resin was then added to the culture, and the cultivation was continued for a further 5 days. The adsorber resin and cell clumps were separated from the medium by sieving, and then extracted with 40 ml of a methanol/acetone mixture (1:1 v/v). The extracts were evaporated to dryness and resuspended in 0.5 ml methanol before analysis by HPLC-MS or LTQ-Orbitrap.

Synthesis of L-*N*-*tert*-butoxycarbonyl-4,5-dideutero-pipecolic acid (L-d_2-Boc-Pip) and D-*N*-*tert*-butoxycarbonyl-4,5-dideutero-pipecolic acid (D-d_2-Boc-Pip)

A solution of *N*-Boc-protected L-4,5-dehydropipecolic acid (186 mg, 0.818 mmol) and Pd/C (10%) catalyst (24 mg) in methanol (10 ml) was stirred under a deuterium atmosphere. When the reaction was finished (TLC control), the catalyst was filtered away using a pad of celite, and the methanol was evaporated to afford L-d_2-Boc-Pip (185 mg, 0.803 mmol, 98% yield) as a white solid (m. p. 104°C). D-d_2-Boc-Pip was obtained by the same method, in quantitative yield.

L-d_2-Boc-Pip: $[\alpha]_D^{20}$ = –45.5 (*c* 1.0, MeOH) [Lit (Johnson et al., 1986): $[\alpha]_D^{24}$ = –45.1 (*c* 1.0, MeOH, L-Boc-Pip)].

D-d_2-Boc-Pip: $[\alpha]_D^{20}$ = +41.2 (*c* 1.0, MeOH) [Lit (Garvey et al., 1992): $[\alpha]_D^{23}$ = +43.6 (*c* 0.96, MeOH, D-Boc-Pip)].

^{1}H-NMR analysis at room temperature showed a 1.7:1 mixture of rotamers. The NMR spectra and mass analysis also indicated that deuteration had occurred to varying extents, yielding a mixture of tri-deuterated (15%), di-deuterated (60%), mono-deuterated (20%), and undeuterated pipecolic acid (7%), in each case. ^{1}H-NMR (400 MHz, $CDCl_3$) (di-deuterated): δ = 1.27 (m, 0.5 H), 1.41 (m, 0.5 H), 1.43 (s, 9 H), 1.56–1.73 (m, 2 H), 2.19 (bs, 1 H), 2.93 (bs, 1 H), 3.90 (d, *J* = 10.8 Hz, 1 H), 4.90 (s, 1 H), 10.00 (bs, 1 H); ^{13}C-NMR (100 MHz, $CDCl_3$): δ = 20.4, 24.3, 26.5, 28.3, 42.0, 53.5, 80.3, 156.2, 177.5; characteristic signals of the minor rotamer: ^{1}H-NMR (400 MHz, $CDCl_3$): δ = 2.89 (bs, 1 H), 3.97 (bs, 1 H), 4.74 (bs, 1 H); ^{13}C-NMR (100 MHz, $CDCl_3$): δ 41.0, 54.7, 155.5, 177.4; HRMS (CI) *m/z* $[M+H]^+$ 232.1519 (calculated for $C_{11}H_{18}D_2NO_4$, 232.1518).

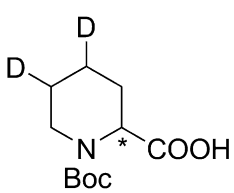

Synthesis of L-4,5-Dideutero-pipecolic acid-hydrochloride (L-d_2-Pip) and D-4,5-Dideutero-pipecolic acid-hydrochloride (D-d_2-Pip)

A solution of HCl in dioxane (4 M, 4 ml, 16 mmol) was added to L-d_2-Boc-Pip (185 mg, 0.803 mmol). When deprotection was complete, the suspension was centrifuged (6000 rpm) for 15 min and the HCl-dioxane solution was decanted off. The product was dried under high-vacuum to yield L-d_2-Pip (107 mg, 0.642 mmol, 78% yield) as a white solid, m. p. 240°C (decomp.). D-d_2-Pip was likewise obtained as a white solid (0.654 mmol, 81% yield). L-d_2-Pip: $[\alpha]_D^{20}$ = –6.3 (*c* 1.0, MeOH), D-d_2-Pip: $[\alpha]_D^{20}$ = +6.2 (*c* 1.0, MeOH). ^{1}H-NMR (400 MHz, D_2O): δ 1.58–1.73 (m, 1 H), 1.78 (m, 1 H), 1.87–1.98 (m, 1 H), 2.31 (dt, *J* = 14.5 Hz, 3.9 Hz, 1 H), 3.06 (m, 1 H), 3.48 (dd, *J* = 12.8 Hz, 3.8 Hz, 1 H), 3.96 (dd, *J* = 11.8 Hz, 3.5 Hz, 1 H); ^{13}C-NMR (100 MHz, D_2O): δ 21.0, 25.7, 43.8, 57.0, 172.0; HRMS (CI) *m/z* $[M+H]^+$ 132.1002 (calculated for $C_6H_{10}D_2NO_2$,132.0993).

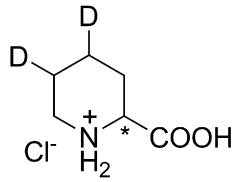

Isolation, Purification and Structure Elucidation of Pretubulysin A

The SBCb004-*tubZ*$^-$ mutant was cultivated in M-medium in the presence of 2% XAD adsorber resin at 30°C for 6 days. Cultivation was carried out in a 17 l fermenter and shaking flasks (9 l; 150 rpm), for a total volume of 26 l. Fermentation was performed with stirring at 300 rpm, an oxygen saturation of 35%, and at a pH of 7.2–7.4. The XAD was separated from the supernatant by sieving. The XAD was then extracted batchwise with a total volume of 6 l methanol. The resulting extracts were combined and evaporated. Before initial purification, the methanolic raw extracts were degreased by counter extraction with heptane. This procedure afforded 18.4 g crude extract.

Initial purification was performed by vacuum liquid chromatography on silica gel, using a stepwise gradient from nonpolar to polar solvents: hexane, chloroform, chloroform/methanol (3:1, 2:1 and 1:1), and methanol. Fractions containing significant amounts of pretubulysin A were combined and evaporated to dryness. Pure pretubulysin A was obtained by purification on a preparative HPLC instrument (Waters), equipped with a 2545 binary gradient module, a 515 HPLC pump, a SFO system fluidics organizer, a 2998 PDA, a 3100 mass detector, and a 2767 sample manager. An X-Bridge RP-C_{18} column (19 × 100 mm, 5 μm) (Waters) was used for separation with a solvent system consisting of water (A) and methanol (B), each containing 0.1% formic acid. The following gradient was applied: 0–0.8 min, 35% B; 0.8–6.8 min 35%–55% B; 6.8–10 min 55%–67.3% B. Fractions were collected using mass-guided fraction collection, with a trigger mass of 686.5 Da. This procedure yielded approximately 6.5 mg of purified pretubulysin A. NMR spectra were recorded on a Bruker Avance 500 spectrometer using CD_3OD as solvent and as an internal standard. For ^{1}H and ^{13}C NMR data, see Table 2.

Isolation of *N*-Desmethyl 12-keto pretubulysin (14)

Wild-type An d48A fermentation was grown in M7-medium (8.5 l) in the presence of 2% Amberlite XAD-16. Fermentation was carried out at 30°C (pH 7.2–7.4, O_2 saturation of 35%, 250 rpm). By HPLC-MS analysis, production of **14** was observed to plateau at day 8, at which point the culture was harvested. The XAD and the cells were separated from the medium by centrifugation, and then stepwise extracted with acetone (1.5 l total) and methanol (3.0 l total). The extracts were filtered, and the solvent removed under vacuum. The remaining 0.3 l aqueous solution was extracted three times with an equal amount of heptane. The water was then removed by freeze-drying to yield 11.2 g of crude extract. The crude extract was fractionated by silica gel-VLC chromatography using a stepwise gradient from nonpolar to polar solvents (hexane, hexane-chloroform (1:1), chloroform, chloroform-methanol (9:1, 3:1, 1:1), methanol, acetonitrile. The resulting fractions were dried under vacuum and analyzed by HPLC-MS. Fractions containing *N*-desmethyl 12-keto pretubulysin (**14**) were pooled, and **14** was purified further by chromatography on a Sephadex LH20 column (100 × 2.5 cm; flow rate 0.083 L/h over 24 h) using

methanol. The fraction containing **14** was applied to a semipreparative HPLC system (Dionex P680 HPLC pump connected to a PDA-100 photo diode array detector; X-Bridge RP-C_{18} column (19 × 100 mm; 5 μm particle diameter, Waters) in a water/acetonitrile gradient (both solvents contained 0.1% formic acid). Chromatographic conditions were: flow rate 10 ml/min; detection wavelengths 210, 254, 366 nm; mobile phase: 35% acetonitrile, 5 min, gradient from 35%–45% acetonitrile, 6 min. This step yielded 1.3 mg of *N*-desmethyl 12-keto pretubulysin (**14**) as a slightly beige amorphous solid.

ACCESSION NUMBERS

The sequence of the tubulysin biosynthetic gene cluster in *Cystobacter* sp. SBCb004 has been deposited in GenBank under accession number GU0002154.

SUPPLEMENTAL INFORMATION

Supplemental Information includes eight figures and one table and can be found with this article online at doi:10.1016/j.chembiol.2010.01.016.

ACKNOWLEDGMENTS

The authors would like to thank Eva Luxenburger, Daniel Krug, and Ole Revermann from the Department of Pharmaceutical Biotechnology for skillful help with various analytical technologies, and Axel Sandmann for assistance with the analysis in vitro of TubZ. We thank Heinrich Steinmetz for provision of synthetic tubulysin D. Work in R.M.'s laboratory is funded by the Bundesministerium für Bildung und Forschung and the Deutsche Forschungsgemeinschaft.

Received: September 30, 2009
Revised: January 21, 2010
Accepted: January 28, 2010
Published: March 25, 2010

REFERENCES

Altmann, K.H., Höfle, G., Müller, R., Mulzer, J., and Prantz, K. (2009). The Epothilones – An Outstanding Family of Anti-Tumour Agents, A.D. Kinghorn, H. Falk, and J. Kobayashi, eds. (New York: Springer).

Altschul, S.F., Madden, T.L., Schaffer, A.A., Zhang, J.H., Zhang, Z., Miller, W., and Lipman, D.J. (1997). Gapped BLAST and PSI-BLAST: a new generation of protein database search programs. Nucleic Acids Res. *25*, 3389–3402.

Balasubramanian, R., Raghavan, B., Steele, J.C., Sackett, D.L., and Fecik, R.A. (2008). Tubulysin analogs incorporating desmethyl and dimethyl tubuphenylalanine derivatives. Bioorg. Med. Chem. Lett. *18*, 2996–2999.

Balasubramanian, R., Raghavan, B., Begaye, A., Sackett, D.L., and Fecik, R.A. (2009). Total synthesis and biological evaluation of tubulysin U, tubulysin V, and their analogues. J. Med. Chem. *52*, 238–240.

Balibar, C.J., Vaillancourt, F.H., and Walsh, C.T. (2005). Generation of D-amino acid residues in assembly of arthrofactin by dual condensation/epimerization domains. Chem. Biol. *12*, 1189–1200.

Banerji, S., and Flieger, A. (2004). Patatin-like proteins: a new family of lipolytic enzymes present in bacteria? Microbiology *150*, 522–525.

Bode, H.B., and Müller, R. (2006). Analysis of myxobacterial secondary metabolism goes molecular. J. Ind. Microbiol. Biotechnol. *33*, 577–588.

Carvalho, R., Reid, R., Viswanathan, N., Gramajo, H., and Julien, B. (2005). The biosynthetic genes for disorazoles, potent cytotoxic compounds that disrupt microtubule formation. Gene *359*, 91–98.

De Crecy-Lagard, V., Marliere, P., and Saurin, W. (1995). Multienzymatic non ribosomal peptide biosynthesis: identification of the functional domains catalysing peptide elongation and epimerisation. C. R. Acad. Sci. III *318*, 927–936.

Dömling, A., and Richter, W. (2005). Myxobacterial epothilones and tubulysins as promising anticancer agents. Mol. Divers. *9*, 141–147.

Dömling, A., Beck, B., Eichelberger, U., Sakamuri, S., Menon, S., Chen, Q.Z., Lu, Y., and Wessjohann, L.A. (2006). Total synthesis of tubulysin U and V. Angew. Chem. Int. Ed. Engl. *45*, 7235–7239.

Dubern, J.F., Coppoolse, E.R., Stiekema, W.J., and Bloemberg, G.V. (2008). Genetic and functional characterization of the gene cluster directing the biosynthesis of putisolvin I and II in *Pseudomonas putida* strain PCL1445. Microbiology *154*, 2070–2083.

Firn, R.D., and Jones, C.G. (2003). Natural products – a simple model to explain chemical diversity. Nat. Prod. Rep. *20*, 382–391.

Garvey, D.S., Wasicak, J.T., Chung, J.Y.L., Shue, Y.K., Carrera, G.M., May, P.D., Mckinney, M.M., Anderson, D., Cadman, E., Vellarountree, L., et al. (1992). Synthesis and *in vitro* characterization of novel amino terminally modified oxotremorine derivatives for brain muscarinic receptors. J. Med. Chem. *35*, 1550–1557.

Gatto, G.J., Boyne, M.T., Kelleher, N.L., and Walsh, C.T. (2006). Biosynthesis of pipecolic acid by RapL, a lysine cyclodeaminase encoded in the rapamycin gene cluster. J. Am. Chem. Soc. *128*, 3838–3847.

Grubbs, R.H., Miller, S.J., and Fu, G.C. (1995). Ring-closing metathesis and related processes in organic synthesis. Acc. Chem. Res. *28*, 446–452.

Johnson, R.L., Rajakumar, G., Yu, K.L., and Mishra, R.K. (1986). Synthesis of Pro-Leu-Gly-NH_2 analogs modified at the prolyl residue and evaluation of their effects on the receptor-binding activity of the central dopamine receptor agonist, ADTN. J. Med. Chem. *29*, 2104–2107.

Kaur, G., Hollingshead, M., Holbeck, S., Schauer-Vukasinovic, V., Camalier, R.F., Domling, A., and Agarwal, S. (2006). Biological evaluation of tubulysin A: a potential anticancer and antiangiogenic natural product. Biochem. J. *396*, 235–242.

Kazmaier, U., and Schneider, C. (1998). Application of the asymmetric chelate enolate Claisen rearrangement to the synthesis of unsaturated polyhydroxylated amino acids. Synthesis, 1321–1326.

Khalil, M.W., Sasse, F., Lünsdorf, H., Elnakady, Y.A., and Reichenbach, H. (2006). Mechanism of action of tubulysin, an antimitotic peptide from myxobacteria. ChemBioChem *7*, 678–683.

Khaw, L.E., Bohm, G.A., Metcalfe, S., Staunton, J., and Leadlay, P.F. (1998). Mutational biosynthesis of novel rapamycins by a strain of *Streptomyces hygroscopicus* NRRL 5491 disrupted in *rapL*, encoding a putative lysine cyclodeaminase. J. Bacteriol. *180*, 809–814.

Kittendorf, J.D., Beck, B.J., Buchholz, T.J., Seufert, W., and Sherman, D.H. (2007). Interrogating the molecular basis for multiple macrolactone ring formation by the pikromycin polyketide synthase. Chem. Biol. *14*, 944–954.

Kopp, M., Irschik, H., Pradella, S., and Müller, R. (2005). Production of the tubulin destabilizer disorazol in *Sorangium cellulosum*: biosynthetic machinery and regulatory genes. ChemBioChem *6*, 1277–1286.

Linne, U., Doekel, S., and Marahiel, M.A. (2001). Portability of epimerization domain and role of peptidyl carrier protein on epimerization activity in nonribosomal peptide synthetases. Biochemistry *40*, 15824–15834.

Luo, L., Kohli, R.M., Onishi, M., Linne, U., Marahiel, M.A., and Walsh, C.T. (2002). Timing of epimerization and condensation reactions in nonribosomal peptide assembly lines: kinetic analysis of phenylalanine activating elongation modules of tyrocidine synthetase B. Biochemistry *41*, 9184–9196.

Margulies, M., Egholm, M., Altman, W.E., Attiya, S., Bader, J.S., Bemben, L.A., Berka, J., Braverman, M.S., Chen, Y.J., Chen, Z., et al. (2005). Genome sequencing in microfabricated high-density picolitre reactors. Nature *437*, 376–380.

Meiser, P., Weissman, K.J., Bode, H.B., Krug, D., Dickschat, J.S., Sandmann, A., and Müller, R. (2008). DKxanthene biosynthesis – understanding the basis for diversity-oriented synthesis in myxobacterial secondary metabolism. Chem. Biol. *15*, 771–781.

Miller, J.F., Termin, A., Koch, K., and Piscopio, A.D. (1998). Stereoselective synthesis of functionalized carbocycles and heterocycles via an ester enolate Claisen/ring-closing metathesis manifold. J. Org. Chem. *63*, 3158–3159.

Moraleda-Munoz, A., and Shimkets, L.J. (2007). Lipolytic enzymes in *Myxococcus xanthus*. J. Bacteriol. *189*, 3072–3080.

Müller, C., Nolden, S., Gebhardt, P., Heinzelmann, E., Lange, C., Puk, O., Welzel, K., Wohlleben, W., and Schwartz, D. (2007). Sequencing and analysis of the biosynthetic gene cluster of the lipopeptide antibiotic friulimicin in *Actinoplanes friuliensis*. Antimicrob. Agents Chemother. *51*, 1028–1037.

Patterson, A.W., Peltier, H.M., Sasse, F., and Ellman, J.A. (2007). Design, synthesis, and biological properties of highly potent tubulysin D analogues. Chemistry *13*, 9534–9541.

Patterson, A.W., Peltier, H.M., and Ellman, J.A. (2008). Expedient synthesis of *N*-methyl tubulysin analogues with high cytotoxicity. J. Org. Chem. *73*, 4362–4369.

Perlova, O., Gerth, K., Hans, A., Kaiser, O., and Müller, R. (2006). Identification and analysis of the chivosazol biosynthetic gene cluster from the myxobacterial model strain *Sorangium cellulosum* So ce56. J. Biotechnol. *121*, 174–191.

Raghavan, B., Balasubramanian, R., Steele, J.C., Sackett, D.L., and Fecik, R.A. (2008). Cytotoxic simplified tubulysin analogues. J. Med. Chem. *51*, 1530–1533.

Rausch, C., Hoof, I., Weber, T., Wohlleben, W., and Huson, D.H. (2007). Phylogenetic analysis of condensation domains in NRPS sheds light on their functional evolution. BMC Evol. Biol. *7*, 78–92.

Rothberg, J.M., and Leamon, J.H. (2008). The development and impact of 454 sequencing. Nat. Biotechnol. *26*, 1117–1124.

Sandmann, A., Sasse, F., and Müller, R. (2004). Identification and analysis of the core biosynthetic machinery of tubulysin, a potent cytotoxin with potential anticancer activity. Chem. Biol. *11*, 1071–1079.

Sani, M., Fossati, G., Huguenot, F., and Zanda, M. (2007). Total synthesis of tubulysins U and V. Angew. Chem. Int. Ed. Engl. *46*, 3526–3529.

Sasse, F., Steinmetz, H., Heil, J., Höfle, G., and Reichenbach, H. (2000). Tubulysins, new cytostatic peptides from myxobacteria acting on microtubuli: production, isolation, physico-chemical and biological properties. J. Antibiot. (Tokyo) *53*, 879–885.

Schneider, C., and Kazmaier, U. (1998). Asymmetric syntheses of chiral allylic alcohols. Synthesis, 1314–1320.

Schuster, M., and Blechert, S. (1997). Olefin metathesis in organic chemistry. Angew. Chem. Int. Ed. Engl. *36*, 2037–2056.

Stachelhaus, T., and Walsh, C.T. (2000). Mutational analysis of the epimerization domain in the initiation module PheATE of gramicidin S synthetase. Biochemistry *39*, 5775–5787.

Steinmetz, H., Glaser, N., Herdtweck, E., Sasse, F., Reichenbach, H., and Höfle, G. (2004). Isolation, crystal and solution structure determination, and biosynthesis of tubulysins—powerful inhibitors of tubulin polymerization from myxobacteria. Angew. Chem. Int. Ed. Engl. *43*, 4888–4892.

Ullrich, A., Chai, Y., Pistorius, D., Elnakady, Y.A., Herrmann, J.E., Weissman, K.J., Kazmaier, U., and Müller, R. (2009). Pretubulysin, a potent and chemically-accessible tubulysin precursor from *Angiococcus disciformis*. Angew. Chem. Int. Ed. Engl. *48*, 4422–4425.

Wang, Z., McPherson, P.A., Raccor, B.S., Balachandran, R., Zhu, G.Y., Day, B.W., Vogt, A., and Wipf, P. (2007). Structure-activity and high-content imaging analyses of novel tubulysins. Chem. Biol. Drug Des. *70*, 75–86.

Weissman, K.J., and Müller, R. (2008). A brief tour of myxobacterial secondary metabolism. Bioorg. Med. Chem. *17*, 2121–2136.

Wenzel, S.C., and Müller, R. (2005). Recent developments towards the heterologous expression of complex bacterial natural product biosynthetic pathways. Curr. Opin. Biotechnol. *16*, 594–606.

Wenzel, S.C., and Müller, R. (2007). Myxobacterial natural product assembly lines: fascinating examples of curious biochemistry. Nat. Prod. Rep. *24*, 1211–1224.

Zumpe, F.L., and Kazmaier, U. (1998). A mild palladium catalyzed *N*-allylation of amino acids and peptides. Synlett, 1199–1200.

Zumpe, F.L., and Kazmaier, U. (1999). Application of the palladium catalyzed *N*-allylation to the modification of amino acids and peptides. Synthesis, 1785–1791.